doi:10.1093/brain/awu380 BRAIN 2015: 138; 679–693 | 679

BRAIN
A JOURNAL OF NEUROLOGY

Subthalamic stimulation modulates cortical motor network activity and synchronization in Parkinson's disease

Daniel Weiss,[1,2,3] Rosa Klotz,[1,2,3] Rathinaswamy B. Govindan,[4] Marlieke Scholten,[1,2,3] Georgios Naros,[3,5] Ander Ramos-Murguialday,[6,7] Friedemann Bunjes,[1,2] Christoph Meisner,[8] Christian Plewnia,[3,9] Rejko Krüger[1,2,3,10] and Alireza Gharabaghi[3,5]

Dynamic modulations of large-scale network activity and synchronization are inherent to a broad spectrum of cognitive processes and are disturbed in neuropsychiatric conditions including Parkinson's disease. Here, we set out to address the motor network activity and synchronization in Parkinson's disease and its modulation with subthalamic stimulation. To this end, 20 patients with idiopathic Parkinson's disease with subthalamic nucleus stimulation were analysed on externally cued right hand finger movements with 1.5-s interstimulus interval. Simultaneous recordings were obtained from electromyography on antagonistic muscles (right flexor digitorum and extensor digitorum) together with 64-channel electroencephalography. Time-frequency event-related spectral perturbations were assessed to determine cortical and muscular activity. Next, cross-spectra in the time-frequency domain were analysed to explore the cortico-cortical synchronization. The time-frequency modulations enabled us to select a time-frequency range relevant for motor processing. On these time-frequency windows, we developed an extension of the phase synchronization index to quantify the global cortico-cortical synchronization and to obtain topographic differentiations of distinct electrode sites with respect to their contributions to the global phase synchronization index. The spectral measures were used to predict clinical and reaction time outcome using regression analysis. We found that movement-related desynchronization of cortical activity in the upper alpha and beta range was significantly facilitated with 'stimulation on' compared to 'stimulation off' on electrodes over the bilateral parietal, sensorimotor, premotor, supplementary-motor, and prefrontal areas, including the bilateral inferior prefrontal areas. These spectral modulations enabled us to predict both clinical and reaction time improvement from subthalamic stimulation. With 'stimulation on', interhemispheric cortico-cortical coherence in the beta band was significantly attenuated over the bilateral sensorimotor areas. Similarly, the global cortico-cortical phase synchronization was attenuated, and the topographic differentiation revealed stronger desynchronization over the (ipsilateral) right-hemispheric prefrontal, premotor and sensorimotor areas compared to 'stimulation off'. We further demonstrated that the cortico-cortical phase synchronization was largely dominated by genuine neuronal coupling. The clinical improvement with 'stimulation on' compared to 'stimulation off' could be predicted from this cortical decoupling with multiple regressions, and the reduction of synchronization over the right prefrontal area showed a linear univariate correlation with clinical improvement. Our study demonstrates wide-spread activity and synchronization modulations of the cortical motor network, and highlights subthalamic stimulation as a network-modulating therapy. Accordingly, subthalamic stimulation may release bilateral cortical computational resources by facilitating movement-related desynchronization. Moreover, the subthalamic nucleus is critical to balance inhibitory and facilitatory cortical players within the motor program.

1 German Centre of Neurodegenerative Diseases (DZNE), 72076 Tübingen, Germany
2 Department for Neurodegenerative Diseases and Hertie Institute for Clinical Brain Research, University of Tübingen, 72076 Tübingen, Germany
3 Werner Reichardt Centre for Integrative Neuroscience, 72076 Tübingen, Germany
4 Foetal Medicine Institute, Division of Foetal and Transitional Medicine, Children's National Health System, M3118C Washington, DC, USA

Received July 28, 2014. Revised October 17, 2014. Accepted November 6, 2014. Advance Access publication January 2, 2015

5 Division of Functional and Restorative Neurosurgery, Department of Neurosurgery, University of Tübingen, 72076 Tübingen, Germany
6 Institute of Medical Psychology and Behavioural Neurobiology, University of Tübingen, 72076 Tübingen, Germany
7 TECNALIA, Health Technologies, 200003 San Sebastian, Spain
8 Clinical Epidemiology and Applied Biometry, University of Tübingen, 72076 Tübingen, Germany
9 Department of Psychiatry and Psychotherapy, Neurophysiology & Interventional Neuropsychiatry, 72076 Tübingen, Germany
10 Clinical and Experimental Neuroscience, Luxembourg Centre for Systems Biomedicine (LCSB), University of Luxembourg and Centre Hospitalier de Luxembourg (CHL), 1210 Luxembourg, Luxembourg

Correspondence to: Daniel Weiss, MD,
Department for Neurodegenerative Diseases and Hertie Institute for Clinical Brain Research,
Department of Neurosurgery,
Centre for Integrative Neuroscience,
University of Tübingen,
Germany
E-mail: daniel.weiss@uni-tuebingen.de

Correspondence may also be addressed to: Alireza Gharabaghi, MD, Division of Functional and Restorative Neurosurgery, Hoppe-Seyler-Str. 3, 72076 Tübingen, Germany E-mail: alireza.gharabaghi@uni-tuebingen.de

Keywords: Parkinson's disease; subthalamic nucleus; deep brain stimulation; synchronization, cortex

Abbreviations: MRD = movement-related desynchronization; STN-DBS = subthalamic nucleus–deep brain stimulation; UPDRS = Unified Parkinson's Disease Rating Scale

Introduction

Dynamic modulations of large-scale network activity and synchronization are inherent to a broad spectrum of cognitive processes (Fell and Axmacher, 2011; Engel *et al.*, 2013). Dysregulation of the concerted interplay in such networks parallels several neuropsychiatric disease states (Uhlhaas and Singer, 2006), and this includes the pathological motor 'off state' in Parkinson's disease (Salenius *et al.*, 2002; Timmermann *et al.*, 2003; Kuhn *et al.*, 2006; Weiss *et al.*, 2012; Hirschmann *et al.*, 2013). Although a comprehensive understanding of neuronal activation and synchronization on the multiple levels of the motor network is still enigmatic (i.e. topography, time, and frequency domain interactions), 'intrinsic coupling modes' were expected to modulate in a context-dependent manner (Engel *et al.*, 2013). Generally speaking, such multilevel organization enables patterning and integration of several consecutive steps and features of processes such as motor integration, including inhibition, relay or execution, and feedback processing to optimize motor performance and behavioural success.

In particular, pathological motor states such as Parkinson's disease are paralleled by excessive synchronization of the basal ganglia—cortical motor network in the beta band, and this may critically interfere with efficient motor integration (Kuhn *et al.*, 2006; Eusebio *et al.*, 2011; Little *et al.*, 2013; Kahan *et al.*, 2014). Consistent with this notion dopaminergic neurodegeneration impacts significant maladaptive activity and connectivity at widely-distributed levels including both subthalamic and motor cortical activity, as well as corticospinal synchronization (Salenius *et al.*, 2002; Kumru *et al.*, 2004; Potter-Nerger *et al.*, 2008; Weiss *et al.*, 2012; Herz *et al.*, 2013). Given that daily life motor function needs rapid and ongoing adjustments of the motor program, it is plausible and supported by experimental evidence that cortical activity and synchronization require short-latency dynamic adjustments. Similarly, a disturbance of these dynamic processes may be of critical relevance for Parkinson's disease motor symptoms as was shown in cortical event-related desynchronization of internally generated movement in Parkinson's disease (Brown and Marsden, 1999; Magnani *et al.*, 2002; Devos *et al.*, 2004).

Here, we set out to study the dynamic large-scale cortical activity and cortico-cortical synchronizations during externally-paced motor processing in patients with Parkinson's disease treated with subthalamic nucleus deep brain stimulation (STN-DBS). We hypothesize that subthalamic stimulation facilitates the movement-related desynchronization (MRD) of cortical activity. With this spectral measure we probe to predict the clinical outcome and reaction time performance from STN-DBS using multiple regression models. Moreover, we apply the time-frequency cross-coherence as a time- and frequency-sensitive measure to characterize the dynamic modulations of cortico-cortical coherence across motor execution. To comprehensively characterize the complex multilevel organization of cortico-cortical synchronization, we use the global synchronization index which quantifies the overall cortico-cortical synchronization. Applying this novel approach we differentiate the complex cortico-cortical synchronization map into 2D topographic representations and demonstrate that our findings were explained by genuine neuronal coupling. Furthermore, we characterize the modulations of cortical motor network synchronization induced by subthalamic stimulation.

Table 1 Clinical characteristics

Patient	Age	Gender	Duration of disease (years)	Duration of DBS (years)	Hoehn and Yahr	LED (mg)
PD1	51	M	11	2	2.5	400
PD2	64	F	16	1	2.5	1210
PD3	52	M	15	3	2	520
PD4	58	M	11	4	2	350
PD5	60	M	15	4	2	150
PD6	55	M	10	1	2	300
PD7	59	M	17	2	3	630
PD8	77	M	7	2	1.5	300
PD9	71	F	26	1	4	200
PD10	53	M	13	4	2	700
PD11	62	F	18	2	4	300
PD12	52	M	16	4	2	300
PD13	52	M	11	1	3	870
PD14	58	M	20	6	4	530
PD15	71	F	22	4	4	750
PD16	51	M	14	5	2	500
PD17	40	M	7	2	2	450
PD18	50	F	21	3	4	680
PD19	75	F	22	6	2	150
PD20	60	M	22	2	4	910

M = male; F = female; LED = L-DOPA equivalent dosage in mg.

Materials and methods

Patients

Twenty-four patients with idiopathic Parkinson's disease and STN-DBS were recorded, and 20 patients were referred for final data analysis (15 male, age 58.6 ± 9.4 years, disease duration 15.7 ± 5.3 years, time with STN-DBS 3.0 ± 1.6 years, all right-handed according to the Edinburgh Handedness Inventory; Table 1). Four patients were excluded from final data analyses: two of them because of reduced EMG quality; one patient did not sufficiently adhere to the experimental paradigm, and one patient did not tolerate the DBS reprogramming and discontinuation of stimulation. All patients were implanted with a quadripolar electrode with iridium contacts (type 3389, Medtronic). Patients were excluded if the Mini-Mental State Examination scored <25 points or if there were other neurological, medical or psychiatric conditions interfering with interpretability of the data. All patients participated with written informed consent and permission of the local ethics committee of the University of Tübingen.

Study experiments were performed after overnight withdrawal of dopaminergic medication. Patients were tested with both 'stimulation off' (StimOff) and bilateral 'stimulation on' (StimOn) in randomized order. Generally, a reliable washout of the clinical DBS effect can be achieved within 30 min after 'switching off DBS' in advanced disease stages as in our cohort (Cooper *et al.*, 2013; Weiss *et al.*, 2013). Motor Unified Parkinson's Disease Rating Scale (UPDRS) III assessments were obtained in each therapeutic condition, and a 'segmental UPDRS III subscore' (items 20–26) was additionally built. Before testing, stimulation parameters were reprogrammed to bipolar settings in case of chronic monopolar stimulation to reduce the DBS artefact in EEG recordings. Therefore, the negative active contact was held constant and polarized against a more dorsal contact. To obtain equivalent clinical efficacy of stimulation, stimulation amplitudes (constant voltage) were increased by 30% after bipolarization as suggested elsewhere (Silberstein *et al.*, 2005; Weiss *et al.*, 2011). Clinical outcome and individual stimulation parameters are given (Table 2).

Paradigm

Patients performed externally paced finger movements of fingers II–V of the right hand that were visually cued in random order with a fixed 1.5-s interstimulus interval. Four red circles were arranged horizontally, and illumination of one of the circles indicated the 'Go' signal for the corresponding finger. Patients were instructed to respond as fast and accurate as possible by button press. Patients were carefully instructed to keep their fingers in permanent contact with the buttons before, during and after a motor response. Adherence to this requirement was monitored online by the investigator. A small-amplitude finger press of ~2 mm was sufficient to elicit the motor response at full depression of the button, and this time-point was registered and referred to as time point '0' for data segmentation. This paradigm was chosen to stabilize the movement characteristics in StimOff and StimOn conditions. A trial was timed-out after 1 s if there was no response. Each patient performed four blocks of 84 random stimuli. In this study, we were interested to study motor integration on externally paced movements with relatively brief interstimulus intervals to be more sensitive for the cortical activation patterns that relate to the direct motor execution process. Similar studies were conducted with interstimulus intervals as short as 500 ms (Gerloff *et al.*, 1998; Herz *et al.*, 2014), and included spectral time-frequency analyses (Hege *et al.*, 2014) using wavelets to avoid standard Fourier transform window length limitation to study low frequencies. We determined reaction time and per cent of correct responses as behavioural motor performance measures.

Electrophysiological recordings

Sixty-four-channel surface EEG was recorded using linked earlobe references and a frontal ground (BrainAmp, Brainproducts). EMG of the right flexor digitorum superficialis and extensor digitorum communis muscles was recorded simultaneously using bipolar, pre-gelled Ag/AgCl surface electrodes (Norotrode, Myotronics-Noromed Inc.). Triggers from 'Go' signals and the subsequent motor responses were registered synchronously to the electrophysiological recording and used for offline data segmentation. EEG and EMG were sampled at 1000 Hz.

Data processing

Before the spectral analyses EEG data were band-pass filtered from 0.5 to 200 Hz and EMG data from 10 to 300 Hz. Afterwards, EMG was full-wave rectified. Both EEG and EMG data were visually inspected and corrected for episodic muscle and movement artefacts. EEG data principal

Table 2 Clinical outcome and individual stimulation parameters

Patient	Segmental UPDRS III (items 20–26)		Left STN	Right STN
	StimOff	StimOn		
PD1	26	6	3–2+, 4.5 V, 60 μs, 130 Hz	7–6+, 4.0 V, 60 μs, 130 Hz
PD2	14	11	2–3+, 3.5 V, 60 μs, 130 Hz	6–7+, 4.2 V, 60 μs, 130 Hz
PD3	25	8	1–2+, 4.3 V, 90 μs, 130 Hz	6–7+, 3.2 V, 90 μs, 130 Hz
PD4	11	2	3–2+, 4.8 V, 60 μs, 130 Hz	7–6+, 4.2 V, 60 μs, 130 Hz
PD5	24	10	2–3+, 5.0 V, 90 μs, 130 Hz	5–6+, 3.5 V, 60 μs, 130 Hz
PD6	12	0	2–1+, 3.5 V, 60 μs, 130 Hz	6–5+, 4.5 V, 90 μs, 130 Hz
PD7	17	7	1–2+, 4.6 V, 60 μs, 120 Hz	5–6+, 4.6 V, 60 μs, 120 Hz
PD8	15	9	2–1+, 6.0 V, 60 μs, 180 Hz	6–5+, 3.0 V, 60 μs, 180 Hz
PD9	29	8	2–3+, 6.5 V, 90 μs, 130 Hz	4–5+, 4.5 V, 60 μs, 130 Hz
PD10	18	2	1–3+, 3.5 V, 60 μs, 130 Hz	6–7+, 2.5 V, 60 μs, 130 Hz
PD11	22	7	2–3+, 5.0 V, 90 μs, 120 Hz	6–7+, 4.5 V, 90 μs, 120 Hz
PD12	17	8	2–3–1+, 4.6 V, 120 μs, 180 Hz	6–5+, 4.0 V, 90 μs, 180 Hz
PD13	7	5	2–3+, 4.2 V, 120 μs, 130 Hz	6–7+, 3.9 V, 120 μs, 130 Hz
PD14	24	8	2–3+, 2.5 V, 60 μs, 130 Hz	6–5+7+, 2.6 V, 120 μs, 130 Hz
PD15	17	9	3–2+, 2.0 V, 120 μs, 125 Hz	7–6+, 2.8 V, 90 μs, 125 Hz
PD16	32	18	1–3+, 4.9 V, 90 μs, 130 Hz	6–7+, 5.2 V, 90 μs, 130 Hz
PD17	24	5	0–3+, 5.6 V, 60 μs, 130 Hz	5–7+, 3.5 V, 120 μs, 130 Hz
PD18	25	16	2–3–1+, 2.7 V, 60 μs,130 Hz	6–7+, 3.9 V, 90 μs, 130 Hz
PD19	18	7	2–3+, 3.3 V, 120 μs, 125 Hz	6–7+, 3.3 V, 120 μs, 125 Hz
PD20	29	16	3–2+, 4.2 V, 60 μs, 130 Hz	6–7+, 3.5 V, 60 μs, 130 Hz

components were extracted using EEGlab and components corresponding to eye blinks, eye movements, frontal or temporal muscle artefacts, or cardiovascular artefacts were removed. Then, the components were transformed back to the channel-by-time series. Finally, reference-free EEG data were obtained using a short Laplacian spatial filter. This step was considered to reduce cortical volume conduction and to improve the spatial resolution of the cortical representations. In this sense, we report our findings by indicating electrode positions that overly neuroanatomic areas of interest or maxima/minima of the spectral topographic distributions. We refer to these representations by indicating cortical areas underlying the electrodes. Data were segmented from −800 ms to +400 ms relative to the registration of the button press at time '0'.

Spectral analyses

Time-frequency measures of cortical activity

To determine the movement-related cortical and muscular activity on the segmented data we computed the event-related spectral perturbation as implemented in EEGlab newtimef function. To obtain better frequency resolution, we used a Hanning-tapered sinusoidal wavelet transform beginning with a three-cycle wavelet that continued to expand slowly and reached half of the cycles on the highest frequency as suggested elsewhere (Delorme and Makeig, 2004). Our approach resulted in a frequency resolution of 2 Hz. We considered a frequency range from 10 to 100 Hz for the muscular spectra (time range: −632 to +232 ms relative to the registration of the finger tap at time '0'), and from 8–100 Hz for the cortical spectra (time range: −591 to +192 ms). Time-frequency samples were normalized on the mean spectral power of the entire epoch at each specific frequency. Statistical procedures on the time-frequency representations are described below.

Time-frequency analysis of cortico-cortical coherence

The event-related cortico-cortical cross-coherence spectra were computed from 10–30 Hz (time range: −632 to +232 ms). The magnitude of cross-coherence varies between 0 and 1 with a value of 0 indicating complete absence of correlation and 1 indicating perfect correlation. We calculated the cortico-cortical cross-coherence between cortical regions of interest, i.e. on electrodes over the bilateral sensorimotor areas ('C3', 'C4'), supplementary motor area ('FCz') and bilateral dorsolateral prefrontal region ('F3', 'F4'). Here, we selected regions of interest to analyse the interhemispheric time-frequency cross-coherence ('C3C4' and 'F3F4'), as well as the cross-coherence over the bilateral sensorimotor areas and both supplementary-motor area ('C3FCz', 'C4FCz') and dorsolateral prefrontal areas ('C3F3', 'C4F4').

Global phase synchronization index and its topographic differentiation

To study the multidimensional cortico-cortical synchronization processes in a more comprehensive way, we introduced the global synchronization index measure. We calculated the pairwise phase synchronization index (ψ) for each pair of electrodes and represented this in a matrix form as an 'association matrix'. We eigenvalue decomposed the association matrix and defined the global synchronization index (γ) as the ratio of the sum of the eigenvalues greater than a

defined tolerance value with respect to the sum of all the eigenvalues. With this definition, γ would take on a value of one in case of perfect synchrony between all possible channels and a value of zero for complete asynchrony between the channels. We obtained the tolerance value using a bootstrap approach (detailed mathematical procedure in the online Supplementary material). To obtain the topographic distribution of the global cortico-cortical synchronization, we identified the electrode sites that contributed significantly to γ based on their eigenvectors (detailed mathematical procedure in the Supplementary material). This was obtained for both the StimOff and StimOn conditions separately. The global synchronization index and its topographic differentiation were applied on the EEG time series of interest after Laplace transform and band-pass filtering for the frequency range of interest. If the global synchronization index was non-zero for a subject on both conditions, we considered these data for further analysis.

We selected three movement-related time windows of interest driven by the results from the spectral time-frequency analyses. The selection of the respective time-series was derived from the muscular activity and cortico-cortical cross-coherence time-frequency analyses, and will be defined along with the result presentation. Together, the procedure allows us to monitor coupling and uncoupling of distinct areas within the global cortical movement-related processing stream on the basis of the phase synchronization index. The detailed mathematical-methodological algorithm is provided in the Supplementary material.

Additionally, we analysed whether phase synchronization in our study represented genuine neuronal synchronization as opposed to the spurious synchronization from non-interacting sources as present in volume conduction. This problem has been discussed as immanent to EEG research and highly non-trivial, and accordingly no general consensus, but several valuable approaches have been put forward in this sense. Of note, most approaches were conceptualized under the premise that volume conduction occurs with zero-phase delay (Nolte *et al.*, 2004; Hipp *et al.*, 2012; Haufe *et al.*, 2013). Therefore, to analyse if the global synchronization index and its topographic differentiation in our study reflected genuine neuronal synchronization, we analysed the phase differences of significant cortico-cortical synchronizations. Briefly, to test this, we assumed that there were three different categories of phase delays in our sequence x, namely (i) values close to zero (<0.1); (ii) values close to pi (pi – pi / 10 to pi + pi / 10); and (iii) all other values, where Category (iii) is compatible with genuine neuronal synchronization as opposed to Categories (i) and (ii) that were expected to reflect instantaneous coupling from non-interacting sources. A detailed mathematical background and statistical consideration on the comparison of the three categories is provided in the Supplementary material.

Statistical analyses

Muscular activity was in part affected by tonic background activity in some patients, i.e. from incomplete relaxation or rigidity, as can be expected in advanced Parkinson's disease stages. To this end, we improved the signal-to-noise ratio by masking the muscular time-frequency samples on the 95% bootstrap significance level with reference to the entire trial epoch, i.e. non-significant muscular activation samples were zeroed out on the individual subject level. This included a correction for multiple comparisons on the multiple time-frequency samples with the false discovery rate. Afterwards, the muscular activation onset was determined from the time-frequency event-related spectral perturbation. We defined the time point of muscular activation onset when activity first exceeded the bootstrap significance level. These onset times were used to compare muscular activation onset of right flexor digitorum superficialis and right extensor digitorum communis muscles between conditions (StimOff versus StimOn) with paired samples *t*-tests. Group level data of muscular activation were obtained as grand averages from these thresholded individual spectra. Clinical and performance measures were compared between conditions using paired samples *t*-tests.

Spectral time-frequency measures of cortical MRD and cortico-cortical cross-coherence were compared between StimOff and StimOn using a non-parametric framework. We determined the Monte-Carlo estimates from the permutation distribution. Permutation statistics were computed for each sample in the time-frequency space as implemented in the Fieldtrip open source toolbox (Oostenveld *et al.*, 2011). We used 1000 random permutations on a dependent samples *t*-test and an adjusted alpha level of $P < 0.025$ per tail. As these sample-wise statistics produce a massive number of comparisons [i.e. the product of the number of channels (64) by times (200) by frequencies (46)], the cluster-based correction method was demonstrated to treat the multiplicity problem effectively without losing sensitivity for spectral modulations (Maris and Oostenveld, 2007).

We used separate multiple regressions to explore whether (i) clinical improvement on the segmental UPDRS motor score; or (ii) reaction time improvement as dependent variables (StimOff minus StimOn) were associated with a change in cortical MRD (StimOff minus StimOn). Therefore, we took the difference in MRD averaged over the time-frequency window of interest (StimOff minus StimOn) as derived from the event-related spectral perturbation analyses. We optimized our model by inserting electrodes placed over the left prefrontal, premotor, supplemental motor, and sensorimotor areas. As MRD may yield similar patterns across neighbouring electrodes, we removed electrodes from the model if there was statistical evidence for collinearity.

The global synchronization index was compared between the StimOff and StimOn conditions using a paired *t*-test with the directed hypothesis that StimOff condition will show higher global phase synchronization than the StimOn condition. A one-tailed $P < 0.05$ was considered statistically significant. To compare the topographic differentiation between StimOff and StimOn, we performed one-tailed paired *t*-tests ($P < 0.05$) on the eigenvector of each cortical channel between the StimOff and StimOn conditions hypothesizing on higher phase synchronization in StimOff than StimOn. We controlled the false positives with the false discovery rate (Benjamini and Hochberg, 1995).

Results

Clinical outcome, performance and muscular activation

StimOn led to a significant improvement of motor symptoms compared to StimOff on the total UPDRS III [22.3 ± 9.7 versus 57.0 ± 13.6; $t(19) = 14.184$, $P < 0.001$]

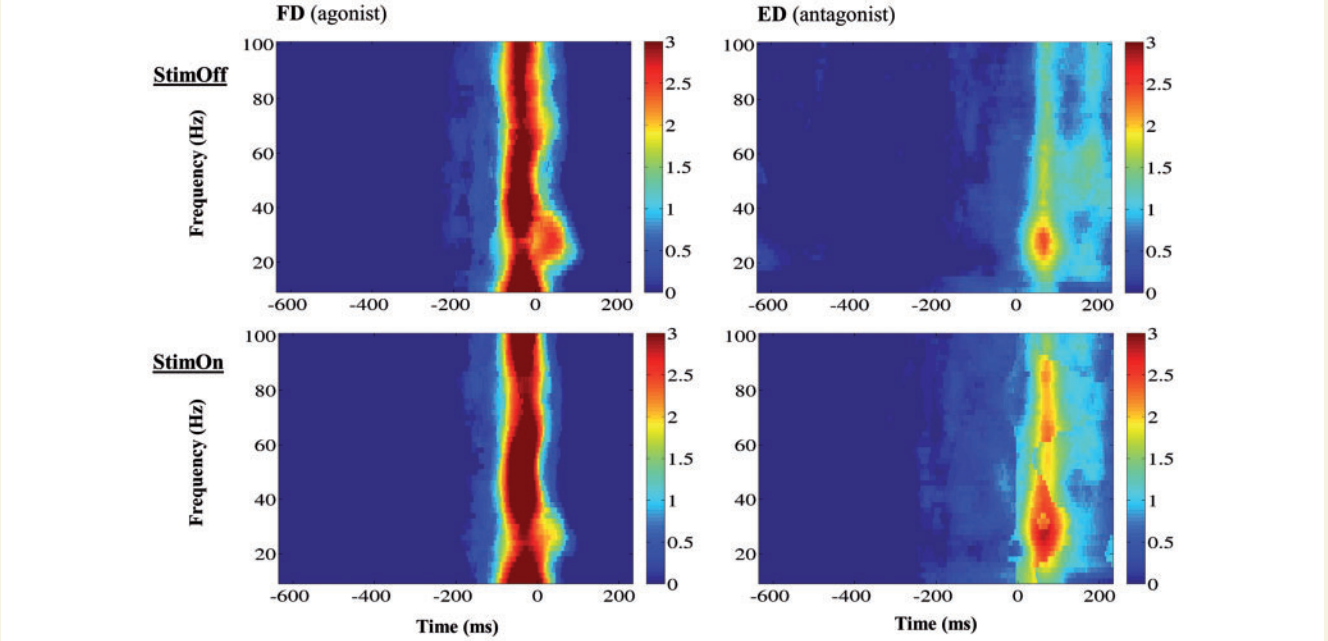

Figure 1 Grand averages of the time-frequency spectra of muscular movement-related spectral pertubations (individual spectra were bootstrap thresholded). No significant differences of M. flexor digitorum (agonist; FD) or M. extensor digitorum (antagonist; ED) activation patterns were found between StimOff and StimOn, i.e. no differences in activation onset, activation strength and frequency response were present, respectively. *x*-axis: Time (ms), where time '0' denotes registration of the finger tap; *y*-axis: Frequency (Hz); activity is coded in colour with warm colours indicating stronger activity (colour bar).

and on the segmental UPDRS III subscore [8.1 ± 4.6 versus 20.3 ± 6.7; $t(19) = 10.532$, $P < 0.001$], as expected. Each patient exhibited an improvement on the total UPDRS III motor score of at least 30% (individual data not shown), and individual improvement of the segmental UPDRS subscore (Table 2). Reaction time was significantly shorter with StimOn compared to StimOff (649.7 ± 137.9 ms versus 712.2 ± 117.0 ms; $P = 0.032$) and the per cent correct responses increased with StimOn compared with StimOff (85.4% ± 14.9 versus 74.8% ± 19.0; $P = 0.016$).

The time course of muscular activation was similar with both StimOff and StimOn (Fig. 1). Right flexor digitorum superficialis muscle activation onset did not differ between therapy conditions [StimOff: −123.5 ± 53 ms, StimOn: −134.7 ± 51 ms; $t(18) = 1.025$, $P = 0.319$]. Right extensor digitorum communis muscle activation onset was similar with −11.0 ± 72 ms with StimOff and −35.3 ± 92 ms with StimOn [$t(17) = 1.017$, $P = 0.324$]. Activation strength and frequency response according to the event-related spectral perturbation of both right flexor digitorum superficialis and right extensor digitorum communis muscles did not differ between StimOff and StimOn conditions both on the raw and the bootstrap-thresholded spectral perturbations.

Movement-related spectral perturbation of cortical activity

In the StimOff condition, alpha (8–12 Hz) and beta band (14–30 Hz) MRD was pronounced on the C3 and C4 electrodes overlying the bilateral sensorimotor areas. This also involved the central and (to a lesser degree) the bilateral frontal electrodes. In the C3 electrode alpha and beta MRD onset occurred at approximately −350 ms relative to fingertap registration at time '0' and outlasted the fingertap for approximately +40 ms. A slight movement-related increase of low and high gamma band activity was observed in the frequency range from 40–80 Hz and from −50 to +70 ms. In StimOn, MRD in the alpha and beta range was significantly stronger compared to StimOff most pronounced over left frontal FC3 and sensorimotor C3 electrodes. Moreover, MRD covered a wider cortical area including the electrodes overlying the bilateral both prefrontal areas (F1, F3, Fz, F2, F9, F10), premotor (FC3, FC4), supplementary-motor (FCz), sensorimotor (C3, C4), and parietal areas (P3, P4). At the left C3 electrode, MRD onset occurred at approximately −350 ms similar to StimOff, however it outlasted the fingertap for +160 ms, and was thereby significantly longer compared with StimOff. There was no difference in gamma activity between conditions. The comprehensive cortical movement-related spectral perturbations are given in Fig. 2.

We conducted several subanalyses to ensure that MRD was significantly modulated by StimOn. First, we ensured that there was no constant suppression of the cortical alpha and beta rhythms throughout the 1.5-s interval. We found that over the C3 electrode of interest, MRD showed significant activity decrease from the epoch mean in both StimOff and StimOn conditions (permutation statistics with $P < 0.05$ including correction for multiple

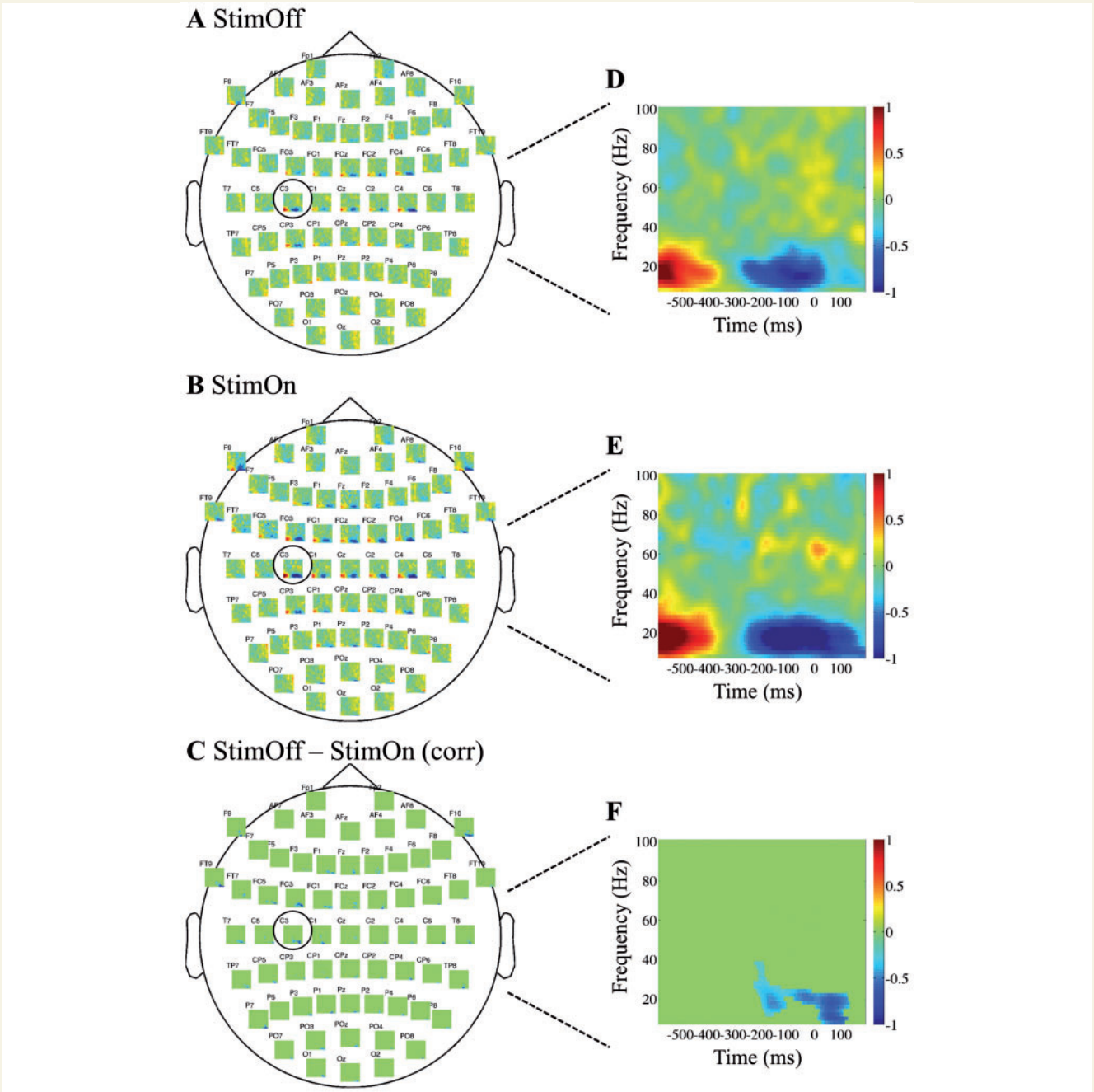

Figure 2 Time-frequency spectra of the cortical movement-related spectral pertubations (multiplots). At each of the 64 electrode positions, a time-frequency plot is given. Grand average spectra of the cortical electrodes are given in StimOff (**A**) and StimOn (**B**), and StimOn minus StimOff (**C**) including the statistical comparison and correction for multiple comparisons using a cluster-based correction method (Maris and Oostenveld, 2007). Non-significant time-frequency samples are 'zeroed out' and given in green. The time-frequency representations of the left sensorimotor region of interest ('C3') are given for StimOff (**D**), StimOn (**E**), and StimOn minus StimOff (**F**). *x*-axis: Time (ms), where time '0' denotes registration of the finger tap; *y*-axis: Frequency (Hz).

comparisons with the false discovery rate). This demonstrates that there was significant movement-related activity modulation and that the task rate did not lead to a continuous and general suppression of the alpha and beta rhythms (not shown). Next, one might argue that StimOn could have introduced a constant decrease of activity between 8–30 Hz. Therefore, we analysed the cortical power spectrum on the entire epoch from −800 to +400 ms and found no significant differences of cortical activity in any of the electrodes (Supplementary Fig. 1). A further important aspect we consider, that higher MRD deflections might arise from higher prestimulus amplitudes (Lemm *et al.*, 2009). Although our experimental paradigm differed from this previous work, we found that cortical activity from

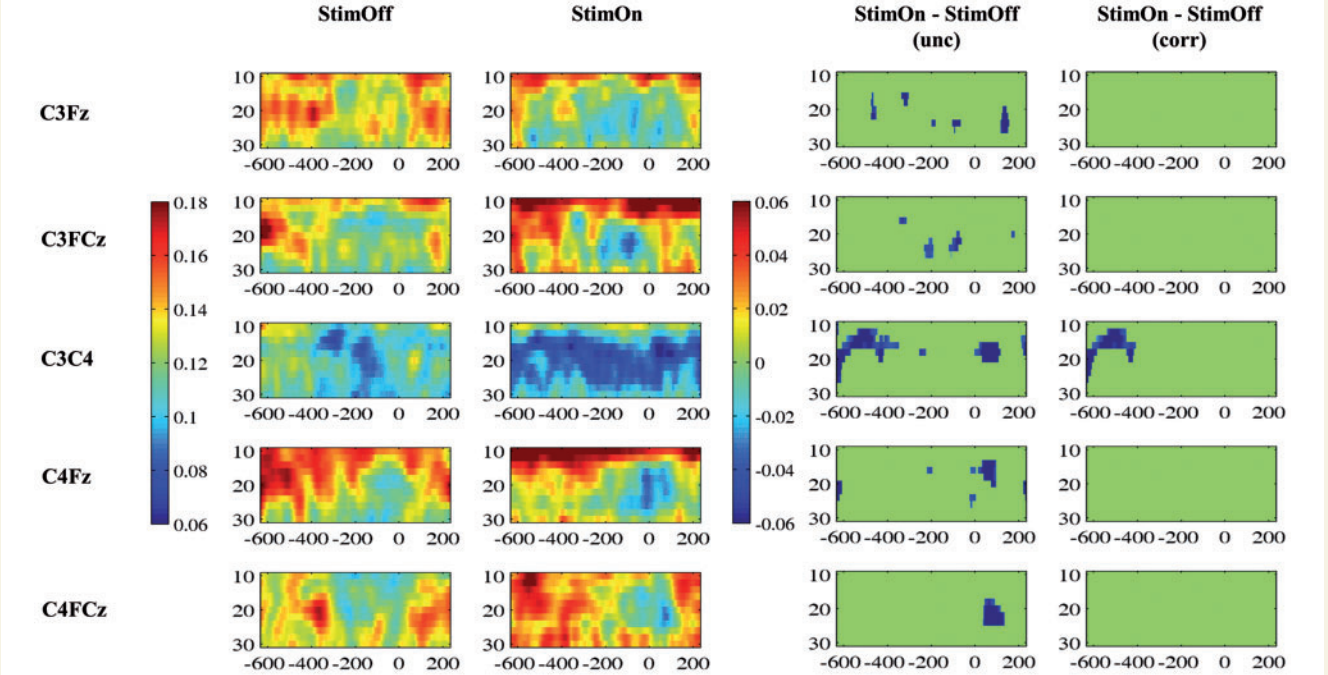

Figure 3 Time-frequency cross-coherence between cortical regions of interest. The first column indicates the grand average spectra in StimOff, the second column in StimOn. The coherence magnitude is indicated by the colour bar (scale from 0.06 to 0.16). As third column, the statistical comparison between StimOff and StimOn (uncorrected) is given, and the fourth column includes correction for multiple comparisons. The difference in coherence magnitude StimOn minus StimOff is indicated by the right colour bar, and non-significant time-frequency samples are 'zeroed out' and masked in green (scaled from 0.06 to −0.06). *x*-axis: Time (ms), where time '0' denotes registration of the finger tap; *y*-axis: Frequency (Hz).

−800 to −400 ms (before MRD onset) and between 8–30 Hz did not show significant differences between StimOff and StimOn in any of the channels (not shown).

We designed the multiple regression model from electrodes over the cortical areas of interest involved in motor integration. We modelled the clinical outcome and reaction time improvement from stimulation from MRD differences between StimOff and StimOn in these cortical areas. For the MRD difference between StimOff and StimOn, we took the mean power of each cortical electrode at the time-frequency window of interest with maximum MRD (frequency range: 14–24 Hz, time range of interest: −198 to −1 ms). We achieved the highest coefficient of determination in predicting UPDRS improvement when applying the five electrodes of interest 'F1', 'FC1', 'FCz', 'C1', 'C5' ($R^2 = 0.61$, $F = 4.293$, $P = 0.014$). Similarly, the reaction time improvement could be modelled with electrodes 'F1', 'FC3', 'Cz', 'C1', 'C5'; ($R^2 = 0.66$, $F = 5.306$, $P = 0.006$).

Cortico-cortical coherence and phase synchronization

The analysis of cortico-cortical time-frequency cross-coherence from 10–30 Hz was considered to explore the characteristics of movement-related coherence. We found movement-related coherence decrease mainly between 'C3FCz', 'C4FCz' and between 'C3F3' pair without significant differences between StimOff and StimOn. This pattern was different in the interhemispheric electrode pairs: both 'F3F4' and 'C3C4' showed a more constant coherence decrease over the whole time range. This was most pronounced in StimOn and reached statistical significance compared to StimOff in the 'C3C4' pair in the premovement phase from −632 to approximately −400 ms (Fig. 3).

For the phase synchronization analysis we selected the frequency range of 14–24 Hz as derived from the significant coherence decrease in 'C3C4'. We selected three time epochs of interest, i.e. the 'premovement period' from −600 to −401 ms which was before cortical MRD and EMG onset; the 'movement period' from −200 to −1 ms, which covered the maximum of cortical MRD, cortico-cortical coherence decrease, and agonist EMG activation; and the early 'postmovement period' from 0 ms to +199 ms. Phase synchronization analysis was considered (i) to analyse neuronal synchronization; and (ii) to analyse the global cortical synchronization as well as distinct cortical contributions to the global cortical synchronization.

The global synchronization index was larger in StimOff compared to StimOn ('premovement period': significant in 12 patients, StimOff > StimOn; $P = 0.0096$; 'movement period': significant in 10 patients, StimOff > StimOn,

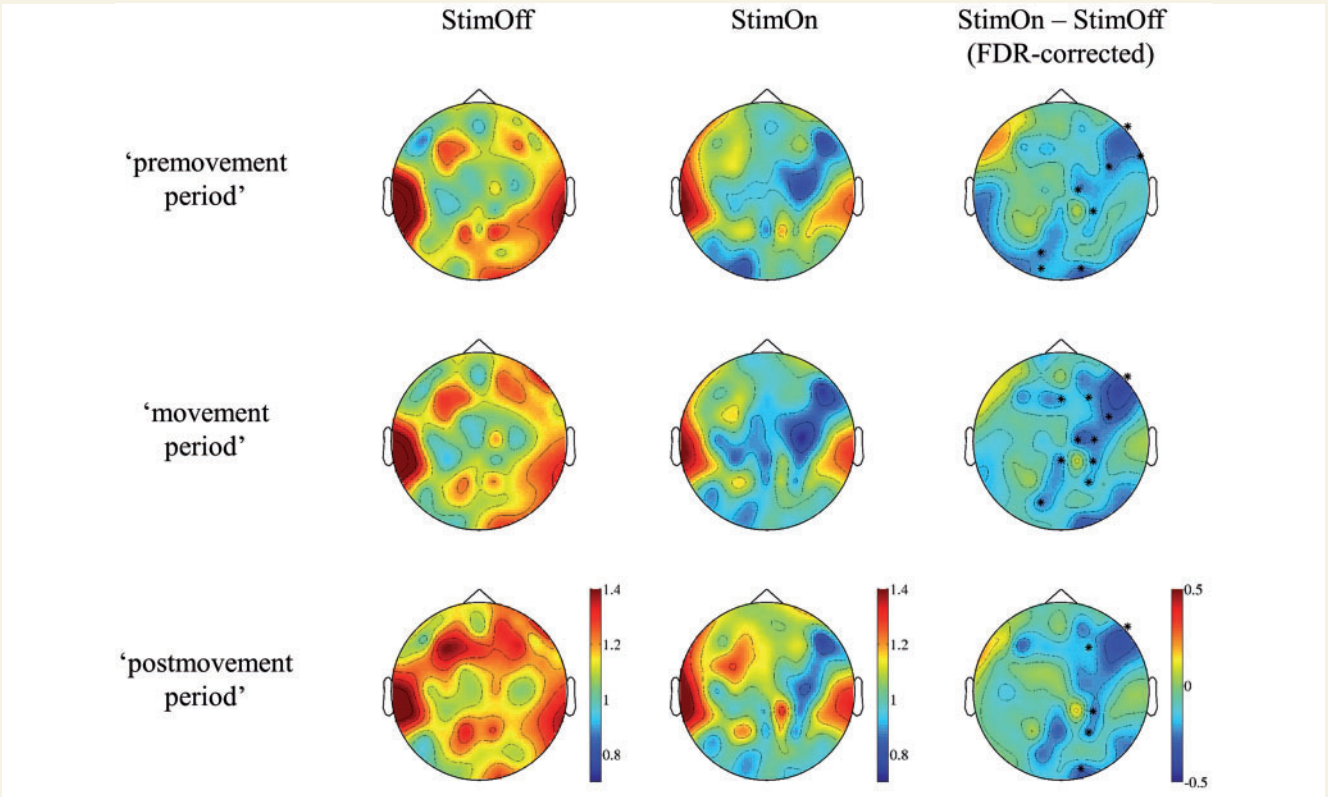

Figure 4 Topographic differentiation of the cortico-cortical phase synchronization in StimOff and StimOn, and difference of StimOn minus StimOff. In the latter column significant desynchronizations between conditions are indicated by asterisks. Colour bars indicate the magnitude of cortico-cortical phase-synchronization with warmer colors indicating stronger phase synchronization.

$P = 0.009$; early 'postmovement period': significant in 10 patients, StimOff > StimOn, $P = 0.021$). The topographic differentiation of cortico-cortical phase synchronization revealed desynchronization over the left fronto-central area in StimOff in both 'premovement period' and 'movement period' (Fig. 4). This was similar in StimOn. As significant difference, we observed a stronger desynchronization over the right prefrontal, premotor, and sensorimotor areas in all three time segments in StimOn compared to StimOff (Fig. 4).

Next, we analysed whether our findings reflected genuine neuronal synchronization. Using Chi-square test, we found that the three categories of phase differences [i.e. (i) values close to zero (<0.1); (ii) values close to pi (pi – pi / 10 to pi + pi / 10); and (iii) all other phase differences] occurred with significantly different proportions ($P < 0.0001$). McNemar's test was used to determine whether the frequencies of occurrences of the categories were equal for each pair of categories. This pairwise test showed that events in Category (iii) were significantly different from Categories (i) or (ii) across all the subjects after adjusting for multiple comparisons ($P < 0.001$). Phase differences in Category (iii) occurred in at least 98% in each single patient with significant phase synchronization. Therefore, the observed phase synchronizations dominantly reflected genuine neuronal synchronization.

The desynchronization over the right prefrontal, premotor, sensorimotor area (electrodes 'F10', 'FC6' and 'C2' predicted clinical improvement on the UPDRS III with a high coefficient of determination in the 'premovement period' ($R^2 = 0.84$, $F = 13.875$, $P = 0.002$), whereas no significant prediction was achieved during the 'movement period' ($R^2 = 0.55$, $F = 2.488$, $P = 0.158$). A linear correlation between UPDRS improvement and the decrease in phase synchronization of the 'F10' electrode was achieved in the 'premovement period' (Pearson's $r = 0.91$, $P < 0.001$; Fig. 5), indicating that clinical improvement correlated with reduced phase synchronization on the right inferior prefrontal area. No significant predictions on the reaction time outcome were obtained from the multiple regressions, however there was a significant correlation of reaction time decrease and synchronization decrease with StimOn compared to StimOff on the 'F10' electrode (Pearson's $r = 0.67$, $P = 0.016$).

Discussion

Here, we demonstrate that subthalamic stimulation modulates both large-scale cortical motor-network activity and synchronization in Parkinson's disease. Our study brought to light several cortical network mechanisms of Parkinson's

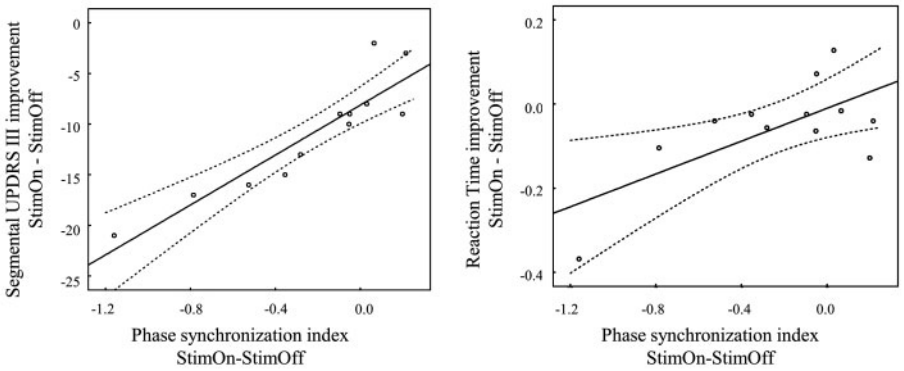

Figure 5 Linear correlation of the topographic differentiation of the global phase synchronization index. Indices are shown for the right inferior prefrontal cortex ('F10' electrode; difference StimOn minus StimOff) and clinical improvement (*left*) in the UPDRS III (StimOn minus StimOff) and reaction time difference (*right*; StimOn minus StimOff) in the 12 patients with significant global phase synchronization in both StimOff and StimOn conditions. The correlations were performed on data from the 'premovement period' in which 12 patients had significant phase synchronization.

disease motor impairment and therapeutic neuromodulation on the level of STN. First, StimOn strengthened the cortical processing by facilitating the MRD in the alpha and beta frequency ranges. With this MRD difference between StimOff and StimOn, we were able to predict both the clinical outcome on the segmental UPDRS III and reaction time improvement in StimOn. The most accurate predictions were achieved when using electrodes over the left sensorimotor, premotor, prefrontal, and midline areas. As further core finding, the cortico-cortical long-range synchronization was significantly decreased with StimOn. This included a reduction of interhemispheric cross-coherence between the bilateral sensorimotor areas, and decreased global phase synchronization in a frequency range between 14–24 Hz. The topographic differentiation pointed to similar desynchronization and resynchronization patterns of phase synchronization on the left (contralateral) hemisphere in both StimOff and StimOn. In contrast, phase synchronization was significantly reduced on electrodes over the right (ipsilateral) prefrontal, premotor, and sensorimotor areas in StimOn compared to StimOff.

Modulation of cortical activity

We found a wide-spread facilitation of cortical MRD with subthalamic nucleus stimulation over the bilateral prefrontal, premotor, supplementary motor, and sensorimotor areas, and this topography complied well with the known cortical connectivity of the STN (Albin *et al.*, 1989; Nambu *et al.*, 1997, 2002). Interestingly, this finding enabled us to predict both clinical and reaction time improvements. Intriguingly, the subthalamic nucleus may facilitate, relay, or inhibit motor cortical processing according to its remote cortical connectivity and, in Parkinson's disease, an over-inhibitory subthalamic tone in the beta frequency range was associated with abnormal motor cortical inhibition and defective corticospinal motor control (Salenius *et al.*, 2002; Kuriakose *et al.*, 2010; Weiss *et al.*, 2012). Our findings are in line with these previous observations. As local subthalamic beta band activity has been shown to be decreased with DBS (Kuhn *et al.*, 2008; Eusebio *et al.*, 2011), and beta band coupling of STN and cortex has been demonstrated particularly in the resting state and during akinesia (Sharott *et al.*, 2005; Weiss *et al.*, 2012), network effects on cortical beta band activity could be assumed during STN-DBS. Accordingly, beta band rhythm modulations may constitute a network-wide mechanism to balance motor execution and inhibition which is considered a core function of the subthalamo-cortical relay (Aron and Poldrack, 2006; Frank, 2006; Weiss *et al.*, 2014). Similarly, the prefrontal cortices are involved in executive motor functions and include response selection in attention-demanding motor skills particularly in motor programs that are not well rehearsed (Jahanshahi, 2013). Accordingly, increase of subthalamic beta band activity was found when conflict responses were inhibited successfully, and the frontal cortex was proposed as the core processor to mediate this motor inhibition presumably via hyperdirect cortico-subthalamic projections (Brittain *et al.*, 2012). Similar evidence for prefrontal contributions came from a PET study on motor timing in Parkinson's disease that found impaired striatal-prefrontal connectivity (Jahanshahi *et al.*, 2010) which improved with dopaminergic therapy (Jahanshahi *et al.*, 2010; Kwak *et al.*, 2010). This impairment to regulate the degree of prefrontal activation in Parkinson's disease (Postuma and Dagher, 2006) probably parallels several executive dysfunctions (Hallett, 2008). It has been postulated that this impairment relates rather to an overinhibitory basal ganglia control on prefrontal activity than to an intrinsic prefrontal dysfunction *per se* (Dirnberger *et al.*, 2005). In line with this consideration, pallidotomy increased prefrontal and supplementary motor activation (Samuel *et al.*, 1997). Our findings add to this view. Given that subthalamic stimulation promotes

movement-related activity decrease of the prefrontal area, this implies remote activity control of the prefrontal cortex and STN. This effect may rather reflect network modulation on remote subthalamic and cortical control than modulation of a single distinct basal ganglia pathway such as the hyperdirect pathway *per se*. The consideration of remote subthalamo-cortical interplay is corroborated by previous findings. It was put forward that STN-cortical modulation by subthalamic neurostimulation occurs on separate pathways in parallel, and that these distributed modulations result in a prokinetic net effect. The most important and reproduced explanations considered a desensitization of STN afferents (including those from the hyperdirect cortico-subthalamic pathway) (Gradinaru *et al*., 2009; Kahan *et al*., 2014), and as a paralleling mechanism remote antidromic motor cortex modulation from subthalamic stimulation was revealed (Li *et al*., 2012; Gradinaru *et al*., 2009). Additionally, cortical activity modulation may occur on the direct pathway, i.e. by facilitating cortical processing on the thalamo-cortical route. In line with our findings it was moreover noted that increases of MRD may reflect a facilitation of thalamo-cortical activation (Steriade and Llinas, 1988; Lemm *et al*., 2009). Together, if an exaggerated inhibitory subthalamic tone (as present in the 'off state') is attenuated with DBS, motor output from the basal ganglia on thalamo-cortical pathways may be facilitated, and conversely, attenuation of cortical beta band activity during motor processing may result in less inhibitory cortical afferents to the STN (e.g. via the hyperdirect pathway with the well-known frontal and central-motor contributions).

Subthalamic stimulation decreases large-scale cortico-cortical coherence and phase synchronization

This study addressed the movement-related modulations of cortico-cortical cross-coherence in Parkinson's disease and its modulation with subthalamic stimulation. Both StimOff and StimOn showed similar movement-related coherence decrease from 14–24 Hz most pronounced on the left hemisphere. This involved the interhemispheric connections, as well as connectivity of the bilateral sensorimotor areas and supplementary motor area. As significant difference, StimOn yielded a stronger and permanent decrease of the interhemispheric coherence between the bilateral sensorimotor areas in the premovement phase. For the phase synchronization analysis we selected a frequency range from 14–24 Hz and three time periods of interest. As core finding, we identified a global reduction of cortico-cortical phase synchronization with StimOn compared to StimOff in all time segments. Next, we provided a comprehensive topographic distribution of cortico-cortical phase-synchronization of distinct cortical regions with respect to their contributions to the global cortical motor network synchronization. Major contributions to cortical desynchronization came from the right (ipsilateral) hemisphere, presumably from the prefrontal, premotor, and sensorimotor areas, and interestingly, this allowed us to model the therapeutic improvement from DBS.

In healthy subjects, interhemispheric (ordinary) coherence between the bilateral sensorimotor areas seems to be tightly associated with motor cortical excitability, as inhibitory 1 Hz repetitive transcranial magnetic stimulation applied to the left hand primary motor representation in healthy subjects resulted in increased interhemispheric coherence between the bilateral motor areas (Strens *et al*., 2002). Similarly, active motor inhibition led to a phasic increase of cortical activity and was paralleled by increased interhemispheric coherence between the bilateral sensorimotor and bifrontal areas (Shibata *et al*., 1998). Adding to these findings in healthy subjects, there is ample evidence on defective interhemispheric inhibition in Parkinson's disease. Cortico-cortical functional connectivity in the alpha and beta bands was pathologically enhanced in early stage Parkinson's disease compared to healthy controls (Olde Dubbelink *et al*., 2013), whereas extensive beta band cortico-cortical coherence characterized the later disease stage (Stoffers *et al*., 2008*a*, *b*). Probably the most intriguing evidence for impaired interhemispheric inhibition in Parkinson's disease comes from pathological mirror movement (Poisson *et al*., 2013; Spagnolo *et al*., 2013). It was discussed that reduced transcallosal inhibition or increased transcallosal facilitation may lead to a less lateralized brain activation, which, in turn could favour the occurrence of mirror movements (Li *et al*., 2007; Poisson *et al*., 2013). Consistent with this, smaller and shorter ipsilateral silent periods indicated impaired interhemispheric inhibition (Spagnolo *et al*., 2013). In the later disease stages, interhemispheric beta band coherence is pathologically increased particularly in the resting state. Interestingly, higher interhemispheric coherence correlated with more advanced motor impairment (Silberstein *et al*., 2005), and this was reduced with both L-DOPA and STN-DBS. Our study adds to this framework by demonstrating that interhemispheric coherence between the bilateral sensorimotor areas was more effectively decreased by STN-DBS in the premovement phase. Finally, this demonstrates the importance of the subthalamic nucleus in regulating the interhemispheric interplay during movement preparation.

Cortico-cortical phase synchronization was substantially desynchronized in StimOn compared to StimOff over the right (ipsilateral) prefrontal, premotor, and sensorimotor areas. Most importantly, this desynchronization predicted the motor improvement on the segmental UPDRS III items most accurately in the 'premovement period', and the reduction in phase synchronization over the right inferior prefrontal area in StimOn compared to StimOff was highly correlated with clinical motor improvement. This indicates that the right prefrontal area may play a critical role in Parkinson's disease motor impairment. Following our findings, an entrainment of the right inferior prefrontal area to motor inhibition can be assumed and was most

pronounced in the 'premovement period'. Further corroborative findings lend support to this view and help to delineate the functionality behind this finding.

Cortico-cortical phase synchronization is considered to reflect neuronal mechanisms to synchronize neurons to a common (cognitive) program, i.e. to 'bind' or to 'hold together' distinct features of a program. Thereby, neuronal synchronization may strengthen information exchange between distributed players during well-defined transient windows in the multidimensional time-frequency-topography space (Fell and Axmacher, 2011). Therefore, we propose that the observed right-hemispheric decrease of phase desynchronization reflects the decoupling of potentially inhibitory cortical processors from the motor program. Inhibitory contributions from these areas can be assumed, as a particular role of the right prefrontal cortex was demonstrated in executive motor control, particularly in 'motor inhibition' (Rubia *et al.*, 2001; Aron *et al.*, 2003; Aron and Poldrack, 2006; Zhang *et al.*, 2012; Hege *et al.*, 2014). Similarly, concordant activation of both STN and the right inferior frontal gyrus were demonstrated during motor response suppression and this pointed to the functional inhibitory synergism of both structures (Aron and Poldrack, 2006). More specific to Parkinson's disease, activity of the right prefrontal area was modulated in Parkinson's disease during repetitive bimanual finger movement in a functional MRI study, i.e. activity decreased in unimpaired movement but increased during involuntary motor blocks. Interestingly, these activity modulations further entrained the right primary motor cortex, dorsal premotor cortex, and the supplementary motor area (Vercruysse *et al.*, 2014), which closely relates to the distributions of the right-hemispheric decrease in phase synchronization in our study.

Methodological considerations

We primarily aimed to study the time period around movement execution instead of a longer premovement planning phase as would have been available during internally generated movement. Therefore, we decided to study externally-paced movement on relatively narrow interstimulus intervals of 1.5 s. This paradigm and the settings of our wavelet analysis led to the limitation that we were not able to study the (post-movement) event-related resynchronization. However, we were able to characterize MRD in narrow-interval externally-paced movement and its modulation with subthalamic stimulation. Studying externally-paced movement is similarly important, as this paradigm closely adheres to the everyday motor demands and requires rapid repetitive motor responses to external triggering. Cortical negativity and connectivity measures were studied on externally paced movements with even much shorter interstimulus intervals of 0.5 s (Gerloff *et al.*, 1998; Herz *et al.*, 2014). Nevertheless, we ensured that the alpha and beta band MRD modulations were significant from epoch mean, which stands against a general suppression of these rhythms in parallel to the relatively rapid task rate. Moreover, we confirmed that StimOn did not lead to a general suppression of the alpha and beta rhythms. Importantly, we also excluded differences in cortical activity before MRD onset as a confounder of our findings as discussed elsewhere (Lemm *et al.*, 2009). Together, these additional analyses substantiate that MRD was facilitated in StimOn.

Our pattern of cortical MRD is in good accordance with previous findings and therefore supports the validity of our analyses including those on cortico-cortical phase synchronization: internally-generated movement MRD occurs over the sensorimotor area contralateral to the intended limb movement during the premovement phase, but becomes largely bilateral and symmetric during the movement execution phase. In Parkinson's disease, internally-generated movements presented with a general impairment of the premovement desynchronization (Magnani *et al.*, 2002), and the mu-rhythm MRD was delayed in Parkinson's disease (Defebvre *et al.*, 1998; Magnani *et al.*, 2002). 'MRD impairment' may emerge and worsen along disease progression (Devos and Defebvre, 2006). Consistent with our findings, one previous study found that the prefrontal MRD mainly occurs in the movement phase and less in the premovement phase of internally-paced movements with both STN-DBS and L-DOPA, but could spread to the premovement phase 'off' therapy (Devos *et al.*, 2004). This corroborates our findings that the prefrontal MRD relates to initiation or delay of the motor command *per se*, i.e. inhibitory versus executive control.

Another important aspect of this study was to ensure that the observed modulations of cortico-cortical phase synchronization indeed reflected genuine neuronal synchronization as opposed to volume conduction from non-interacting sources (Nolte *et al.*, 2004; Hipp *et al.*, 2012; Haufe *et al.*, 2013). We demonstrated that the phase differences in our study were largely dominated by genuine synchronization but significantly different from volume conductions characteristics.

Stimulation artefacts were limited although not absent by using bipolar DBS configurations. We found that DBS caused a sharp artefact at the stimulation frequency itself and on harmonic frequencies. Importantly, however, we verified that the individual power spectra were not affected in the major frequency range of interest below 30 Hz. Moreover, the statistical comparisons of StimOff and StimOn confirmed that cortical activity was not affected by DBS (spectra in StimOff and StimOn presented as Supplementary Fig. 1).

Taken together, our study identifies important mechanisms of subthalamic stimulation on cortical network processes. Two major mechanisms were demonstrated, in that subthalamic stimulation facilitates MRD, and decouples potentially motor inhibitory cortical processors from the global motor network processing stream during motor preparation and motor execution. The present findings contribute to a more comprehensive understanding of the

large-scale motor network effects of subthalamic neurostimulation and raise attractive novel candidate regions and biomarkers for future neuromodulation strategies.

Acknowledgements

We would like to thank Dr R. B. Lenin for statistical guidance (Department of Mathematics, University of Central Arkansas, Conway, AR, USA).

Funding

Daniel Weiss is supported by a research grant of the German Research Council (DFG) WE5375/1-1 and was supported by a Research Grant of the Medical Faculty of the University of Tübingen (AKF 259-0-0). Daniel Weiss received speaker's honoraria and a travel grant from Medtronic, Abott Pharmaceutical, UCB, and the Movement Disorder Society. Christian Plewnia received research grants from the German Research Council (DFG; PL 525/1–1), the University of Tübingen (AKF #238-0-0) and the Werner Reichardt Centre for Integrative Neuroscience (CIN, PP2011_11). He received speaker's honoraria by Inomed Medizintechnik GmbH. Rejko Krüger serves as Editor of European Journal of Clinical Investigation, Journal of Neural Transmission and Associate Editor of BMC Neurology; has received research grants of the Fonds National de Recherche de Luxembourg (FNR; PEARL), German Research Council (DFG; KR2219/2-3 and KR2119/8-1), the Michael J Fox Foundation, the Fritz Thyssen foundation (10.11.2.153) and the Federal Ministry for Education and Research [BMBF, COURAGE-PD and Mito-PD], as well as speaker's honoraria and/or travel grants from UCB Pharma, Abbvie, St. Jude Medicals, and Medtronic.

Alireza Gharabaghi is supported by grants from the German Research Council [DFG EC 307], and the Federal Ministry for Education and Research [BFNT 01GQ0761, BMBF 16SV3783, BMBF 03160064B, BMBF V4UKF014. Alireza Gharabaghi received speaker's honoraria and travel grants from Medtronic.

Supplementary material

Supplementary material is available at *Brain* online.

References

Albin RL, Young AB, Penney JB. The functional anatomy of basal ganglia disorders. Trends Neurosci 1989; 12: 366–75.

Aron AR, Fletcher PC, Bullmore ET, Sahakian BJ, Robbins TW. Stop-signal inhibition disrupted by damage to right inferior frontal gyrus in humans. Nat Neurosci 2003; 6: 115–6.

Aron AR, Poldrack RA. Cortical and subcortical contributions to Stop signal response inhibition: role of the subthalamic nucleus. J Neurosci 2006; 26: 2424–33.

Benjamini YH, Hochberg Y. Controlling the false discovery rate: a practical and powerful approach to multiple testing. J R Stat Soc Ser B Stat Methodol 1995: 289–300.

Brittain JS, Watkins KE, Joundi RA, Ray NJ, Holland P, Green AL, et al. A role for the subthalamic nucleus in response inhibition during conflict. J Neurosci 2012; 32: 13396–401.

Brown P, Marsden CD. Bradykinesia and impairment of EEG desynchronization in Parkinson's disease. Mov Disord 1999; 14: 423–9.

Cooper SE, McIntyre CC, Fernandez HH, Vitek JL. Association of deep brain stimulation washout effects with Parkinson disease duration. JAMA Neurol 2013; 70: 95–9.

Defebvre L, Bourriez JL, Derambure P, Duhamel A, Guieu JD, Destee A. Influence of chronic administration of L-DOPA on event-related desynchronization of mu rhythm preceding voluntary movement in Parkinson's disease. Electroencephalogr Clin Neurophysiol 1998; 109: 161–7.

Delorme A, Makeig S. EEGLAB: an open source toolbox for analysis of single-trial EEG dynamics including independent component analysis. J Neurosci Methods 2004; 134: 9–21.

Devos D, Defebvre L. Effect of deep brain stimulation and L-Dopa on electrocortical rhythms related to movement in Parkinson's disease. Prog Brain Res 2006; 159: 331–49.

Devos D, Labyt E, Derambure P, Bourriez JL, Cassim F, Reyns N, et al. Subthalamic nucleus stimulation modulates motor cortex oscillatory activity in Parkinson's disease. Brain 2004; 127(Pt 2): 408–19.

Dirnberger G, Frith CD, Jahanshahi M. Executive dysfunction in Parkinson's disease is associated with altered pallidal-frontal processing. Neuroimage 2005; 25: 588–99.

Engel AK, Gerloff C, Hilgetag CC, Nolte G. Intrinsic coupling modes: multiscale interactions in ongoing brain activity. Neuron 2013; 80: 867–86.

Eusebio A, Thevathasan W, Doyle Gaynor L, Pogosyan A, Bye E, Foltynie T, et al. Deep brain stimulation can suppress pathological synchronisation in parkinsonian patients. J Neurol Neurosurg Psychiatry 2011; 82: 569–73.

Fell J, Axmacher N. The role of phase synchronization in memory processes. Nat Rev Neurosci 2011; 12: 105–18.

Frank MJ. Hold your horses: a dynamic computational role for the subthalamic nucleus in decision making. Neural Netw 2006; 19: 1120–36.

Gradinaru V, Mogri M, Thompson KR, Henderson JM, Deisseroth K. Optical deconstruction of parkinsonian neural circuitry. Science 2009; 324: 354–9.

Gerloff C, Uenishi N, Nagamine T, Kunieda T, Hallett M, Shibasaki H. Cortical activation during fast repetitive finger movements in humans: steady-state movement-related magnetic fields and their cortical generators. Electroencephalogr Clin Neurophysiol 1998; 109: 444–53.

Hallett M. The intrinsic and extrinsic aspects of freezing of gait. Mov Disord 2008; 23(Suppl 2): S439–43.

Haufe S, Nikulin VV, Muller KR, Nolte G. A critical assessment of connectivity measures for EEG data: a simulation study. Neuroimage 2013; 64: 120–33.

Hege MA, Preissl H, Stingl KT. Magnetoencephalographic signatures of right prefrontal cortex involvement in response inhibition. Hum Brain Mapp 2014.

Herz DM, Siebner HR, Hulme OJ, Florin E, Christensen MS, Timmermann L. Levodopa reinstates connectivity from prefrontal to premotor cortex during externally paced movement in Parkinson's disease. Neuroimage 2013; 90C: 15–23.

Herz DM, Siebner HR, Hulme OJ, Florin E, Christensen MS, Timmermann L. Levodopa reinstates connectivity from prefrontal

to premotor cortex during externally paced movement in Parkinson's disease. Neuroimage 2014; 90: 15–23.
Hipp JF, Hawellek DJ, Corbetta M, Siegel M, Engel AK. Large-scale cortical correlation structure of spontaneous oscillatory activity. Nat Neurosci 2012; 15: 884–90.
Hirschmann J, Ozkurt TE, Butz M, Homburger M, Elben S, Hartmann CJ, et al. Differential modulation of STN-cortical and cortico-muscular coherence by movement and levodopa in Parkinson's disease. Neuroimage 2013; 68: 203–13.
Jahanshahi M. Effects of deep brain stimulation of the subthalamic nucleus on inhibitory and executive control over prepotent responses in Parkinson's disease. Front Syst Neurosci 2013; 7: 118.
Jahanshahi M, Jones CR, Zijlmans J, Katzenschlager R, Lee L, Quinn N, et al. Dopaminergic modulation of striato-frontal connectivity during motor timing in Parkinson's disease. Brain 2010; 133 (Pt 3): 727–45.
Kahan J, Urner M, Moran R, Flandin G, Marreiros A, Mancini L, et al. Resting state functional MRI in Parkinson's disease: the impact of deep brain stimulation on 'effective' connectivity. Brain 2014; 137 (Pt 4): 1130–44.
Kuhn AA, Kempf F, Brucke C, Gaynor Doyle L, Martinez-Torres I, Pogosyan A, et al. High-frequency stimulation of the subthalamic nucleus suppresses oscillatory beta activity in patients with Parkinson's disease in parallel with improvement in motor performance. J Neurosci 2008; 28: 6165–73.
Kuhn AA, Kupsch A, Schneider GH, Brown P. Reduction in subthalamic 8-35 Hz oscillatory activity correlates with clinical improvement in Parkinson's disease. Eur J Neurosci 2006; 23: 1956–60.
Kumru H, Summerfield C, Valldeoriola F, Valls-Sole J. Effects of subthalamic nucleus stimulation on characteristics of EMG activity underlying reaction time in Parkinson's disease. Mov Disord 2004; 19: 94–100.
Kuriakose R, Saha U, Castillo G, Udupa K, Ni Z, Gunraj C, et al. The nature and time course of cortical activation following subthalamic stimulation in Parkinson's disease. Cereb Cortex 2010; 20: 1926–36.
Kwak Y, Peltier S, Bohnen NI, Muller ML, Dayalu P, Seidler RD. Altered resting state cortico-striatal connectivity in mild to moderate stage Parkinson's disease. Front Syst Neurosci 2010; 4: 143.
Lemm S, Muller KR, Curio G. A generalized framework for quantifying the dynamics of EEG event-related desynchronization. PLoS Comput Biol 2009; 5: e1000453.
Li JY, Espay AJ, Gunraj CA, Pal PK, Cunic DI, Lang AE, et al. Interhemispheric and ipsilateral connections in Parkinson's disease: relation to mirror movements. Mov Disord 2007; 22: 813–21.
Li Q, Ke Y, Chan DC, Qian ZM, Yung KK, Ko H, et al. Therapeutic deep brain stimulation in Parkinsonian rats directly influences motor cortex. Neuron 2012; 76: 1030–41.
Little S, Pogosyan A, Neal S, Zavala B, Zrinzo L, Hariz M, et al. Adaptive deep brain stimulation in advanced Parkinson disease. Ann Neurol 2013; 74: 449–57.
Magnani G, Cursi M, Leocani L, Volonte MA, Comi G. Acute effects of L-dopa on event-related desynchronization in Parkinson's disease. Neurol Sci 2002; 23: 91–7.
Maris E, Oostenveld R. Nonparametric statistical testing of EEG- and MEG-data. J Neurosci Methods 2007; 164: 177–90.
Nambu A, Tokuno H, Inase M, Takada M. Corticosubthalamic input zones from forelimb representations of the dorsal and ventral divisions of the premotor cortex in the macaque monkey: comparison with the input zones from the primary motor cortex and the supplementary motor area. Neurosci Lett 1997; 239: 13–6.
Nambu A, Tokuno H, Takada M. Functional significance of the cortico-subthalamo-pallidal 'hyperdirect' pathway. Neurosci Res 2002; 43: 111–7.
Nolte G, Bai O, Wheaton L, Mari Z, Vorbach S, Hallett M. Identifying true brain interaction from EEG data using the imaginary part of coherency. Clin Neurophysiol 2004; 115: 2292–307.
Olde Dubbelink KT, Stoffers D, Deijen JB, Twisk JW, Stam CJ, Hillebrand A, et al. Resting-state functional connectivity as a marker of disease progression in Parkinson's disease: A longitudinal MEG study. Neuroimage Clin 2013; 2: 612–9.
Oostenveld R, Fries P, Maris E, Schoffelen JM. FieldTrip: open source software for advanced analysis of MEG, EEG, and invasive electrophysiological data. Comput Intell Neurosci 2011; 2011: 156869.
Poisson A, Ballanger B, Metereau E, Redoute J, Ibarolla D, Comte JC, et al. A functional magnetic resonance imaging study of pathophysiological changes responsible for mirror movements in Parkinson's disease. PLoS One 2013; 8: e66910.
Postuma RB, Dagher A. Basal ganglia functional connectivity based on a meta-analysis of 126 positron emission tomography and functional magnetic resonance imaging publications. Cereb Cortex 2006; 16: 1508–21.
Potter-Nerger M, Ilic TV, Siebner HR, Deuschl G, Volkmann J. Subthalamic nucleus stimulation restores corticospinal facilitation in Parkinson's disease. Mov Disord 2008; 23: 2210–5.
Rubia K, Russell T, Overmeyer S, Brammer MJ, Bullmore ET, Sharma T, et al. Mapping motor inhibition: conjunctive brain activations across different versions of go/no-go and stop tasks. Neuroimage 2001; 13: 250–61.
Salenius S, Avikainen S, Kaakkola S, Hari R, Brown P. Defective cortical drive to muscle in Parkinson's disease and its improvement with levodopa. Brain 2002; 125(Pt 3): 491–500.
Samuel M, Ceballos-Baumann AO, Turjanski N, Boecker H, Gorospe A, Linazasoro G, et al. Pallidotomy in Parkinson's disease increases supplementary motor area and prefrontal activation during performance of volitional movements an H2(15)O PET study. Brain 1997; 120(Pt 8): 1301–13.
Sharott A, Magill PJ, Harnack D, Kupsch A, Meissner W, Brown P. Dopamine depletion increases the power and coherence of beta-oscillations in the cerebral cortex and subthalamic nucleus of the awake rat. Eur J Neurosci 2005; 21: 1413–22.
Shibata T, Shimoyama I, Ito T, Abla D, Iwasa H, Koseki K, et al. The synchronization between brain areas under motor inhibition process in humans estimated by event-related EEG coherence. Neurosci Res 1998; 31: 265–71.
Silberstein P, Pogosyan A, Kuhn AA, Hotton G, Tisch S, Kupsch A, et al. Cortico-cortical coupling in Parkinson's disease and its modulation by therapy. Brain 2005; 128(Pt 6): 1277–91.
Spagnolo F, Coppi E, Chieffo R, Straffi L, Fichera M, Nuara A, et al. Interhemispheric balance in Parkinson's disease: a transcranial magnetic stimulation study. Brain Stimul 2013; 6: 892–7.
Steriade M, Llinas RR. The functional states of the thalamus and the associated neuronal interplay. Physiol Rev 1988; 68: 649–742.
Stoffers D, Bosboom JL, Deijen JB, Wolters E, Stam CJ, Berendse HW. Increased cortico-cortical functional connectivity in early-stage Parkinson's disease: an MEG study. Neuroimage 2008a; 41: 212–22.
Stoffers D, Bosboom JL, Wolters E, Stam CJ, Berendse HW. Dopaminergic modulation of cortico-cortical functional connectivity in Parkinson's disease: an MEG study. Exp Neurol 2008b; 213: 191–5.
Strens LH, Oliviero A, Bloem BR, Gerschlager W, Rothwell JC, Brown P. The effects of subthreshold 1 Hz repetitive TMS on cortico-cortical and interhemispheric coherence. Clin Neurophysiol 2002; 113: 1279–85.
Timmermann L, Gross J, Dirks M, Volkmann J, Freund HJ, Schnitzler A. The cerebral oscillatory network of parkinsonian resting tremor. Brain 2003; 126(Pt 1): 199–212.
Uhlhaas PJ, Singer W. Neural synchrony in brain disorders: relevance for cognitive dysfunctions and pathophysiology. Neuron 2006; 52: 155–68.
Vercruysse S, Spildooren J, Heremans E, Wenderoth N, Swinnen SP, Vandenberghe W, et al. The neural correlates of upper limb motor

blocks in Parkinson's disease and their relation to freezing of gait. Cereb Cortex 2014; 24: 3154–66.

Weiss D, Breit S, Hoppe J, Hauser AK, Freudenstein D, Kruger R, et al. Subthalamic nucleus stimulation restores the efferent cortical drive to muscle in parallel to functional motor improvement. Eur J Neurosci 2012; 35: 896–908.

Weiss D, Govindan RB, Rilk A, Wachter T, Breit S, Zizlsperger L, et al. Central oscillators in a patient with neuropathic tremor: evidence from intraoperative local field potential recordings. Mov Disord 2011; 26: 323–7.

Weiss D, Lam JM, Breit S, Gharabaghi A, Kruger R, Luft AR, et al. The subthalamic nucleus modulates the early phase of probabilistic classification learning. Exp Brain Res 2014; 232: 2255–62.

Weiss D, Walach M, Meisner C, Fritz M, Scholten M, Breit S, et al. Nigral stimulation for resistant axial motor impairment in Parkinson's disease? A randomized controlled trial. Brain 2013; 136(Pt 7): 2098–108.

Zhang J, Hughes LE, Rowe JB. Selection and inhibition mechanisms for human voluntary action decisions. Neuroimage 2012; 63: 392–402.